Validation of the High-Resolution Sea State Forecast Model CWAM using Satellite-based Radar Measurements

Andrey L. Pleskachevsky [a], *Susanne Lehner* [a], *Claus Gebhardt* [a], *Wolfgang Rosenthal* [a], *Jens Kieser* [b], *Thomas Bruns* [b], *Peter Hoffmann* [b], *Egbert Schwarz* [c], *Detmar Krause* [c]

[a] German Aerospace Center (DLR), Remote Sensing Technology Institute, Maritime Security Lab, Henrich-Focke-Straße 4, 28199 Bremen, Germany
Andrey.Pleskachevsky@dlr.de, Susanne.Lehner@dlr.de, Claus.Gebhardt@dlr.de, Wolfgang.Rosenthal@dlr.de

[b] German Meteorological Service (DWD), Bernhard-Nocht-Str. 76, 20359 Hamburg, Germany
Jens.Kieser@dwd.de, Thomas.Bruns@dwd.de, Peter.Hoffmann@dwd.de

[c] German Aerospace Center (DLR), German Remote Sensing Data Center, National Ground Segment Kalkhorstweg 53, 17235 Neustrelitz, Germany
Egbert.Schwarz@dlr.de, Detmar.Krause@dlr.de

Abstract

In order to validate the new coastal forecast model of German Weather Service's (DWD) CWAM (Coastal WAve Model) with 900m horizontal resolution in the German Bight of the North Sea the remote sensing Synthetic Aperture Radar (SAR) data from TerraSAR-X and Tandem-X (TS-X and TD-X) satellites have been used.

The sea state parameters were estimated using the empirical XWAVE_C (C=Coastal) algorithm adopted for coastal regions in Wadden seas with specific short sea state and integrated into Sea State Processor (SSP) for fully automatic processing. The algorithm is based on the spectral analysis of subscenes and the model function uses integrated image spectra parameters as well as local wind information from the subscene analyzed. The algorithm is able to recognize and remove the influence of not sea state produced signals in Wadden sea areas like dry sandbars as well as nonlinear SAR image distortions produced by e.g. short wind waves and wave breaking. Also parameters of very short waves, which are not visible in SAR images and produce only clutter, can be estimated. The SSP includes XWAVE_C, a pre-filtering procedure for removing artefacts like ships, seamarks, buoys, offshore constructions and slicks and an additional procedure performing a control of results based on the statistics of the whole scene. The SSP allows an automatic processing of TS-X images with an error RMSE=25cm and Scatter Index SI=20% for total significant wave height H_S from sequences of TS-X StripMap images with a coverage of ~30km×300km across the German Bight in comparison to 6 available buoys.

The collected, processed and analyzed data base for the German Bight consists of more than 60 TS-X StripMap scenes/overflights with more than 200 images since 2013 with sea state of H_S=0-7m with a mean value of 1.25m over all available scenes at buoy locations. The comparisons with results of the wave prediction model show a number of local variations due to variety in bathymetry and wind fronts.

SSP was implemented into processing chain and tested for Near Real Time (NRT) services in the DLR Ground Station "Neustrelitz". For the common users, a file with the data (lon, lat, H_S), the Google Earth file (.kmz) to preview the image file (.jpg) with color-coded wave heights are provided.

1. Introduction

The paper introduces an algorithm and processor for meteo-marine parameter estimation from TerraSAR-X satellite imagery for practical applications. In the current **Section 1**, the general background, data used and forecast model are reviewed, the methodology is described in **Section 2**. **Section 3** is dedicated to Sea State Processor for practical use. The example of data processing and results are summarized in **Section 4**. The paper is addressed in the first place to the SAR oceanography community and to users of remote sensing data like meteorological services.

1. 1. Radar satellite-borne based techniques for maritime applications

The estimation of marine and meteorological parameters is an important task for operational oceanographic services. In comparison to *in-situ* buoy measurements at a single location, remote sensing allows to cover large areas and to estimate the spatial distribution of investigated parameters. The spatial validation of forecast data, e.g. sea state and surface wind, by remote sensing can visibly improve the forecast quality and help explain natural phenomena beyond

ordinary circumstances like storm front propagation, local wind gusts and occurrence of wave groups with extreme wave height (Lehner et al., 2012, 2013). Ocean surface measurements by SAR have been done since the first space borne SAR missions in 1971. This includes such well-known missions as L-band SAR SEASAT launched in 1978, C-Band European Radar Satellites ERS-1 and ERS-2 launched in 1991 and 1995, ENVISAT (Environmental Satellite) with C-Band Advanced Synthetic Aperture Radar (ASAR) in 2002 and other (Hasselman et al., 2012).

Dependent on resolution and coverage, the remote sensing data can be used in three ways:

(1) Comparison of the data with already simulated processes (hindcast) to study different weather conditions (e.g. storms) in order to improve the model physics and parametrization.
(2) Validation of the forecast: the data are NRT processed and immediately transferred to weather services to be displayed together with the actual forecast minutes after the acquisition for comparisons.
(3) Assimilation of the data in the model runs: the sea state forecast model input is modified using the remote sensing data.

For example, it was shown that wave groups with abnormal height in the North Sea are connected to atmospheric effects observed in SAR images. It turned out that they are caused by mesoscale wind gust that are moving as an organized system across the sea and "drag" the continuously growing waves (Pleskachevsky et al., 2012). According to ASAR (Advanced Synthetic Aperture Radar onboard ENVISAT) measurements, the footprints of mesoscale cloud patterns, observed in optical satellite images (hexagon-ring patterns with a diameter of 30km-90km associated with so-called *open cells* due to convection in the atmosphere during cold air outbreaks), produce a local increase in the wind field at the sea surface with a sharp gradient along their leading edge. Synergetic use of data from different SAR satellites acquired in 30min apart (ERS-2 and ASAR) shows a continuous moving of the individual gusts as a system and allows estimating their propagation speed. The local impact of these gusts on the ocean waves increases significantly if the gust propagation speed is close to the speed of the wave groups. Strong wind energy feeding the same group for a longer time period causes a growth of the individual wave within the group and results in a resonance. The parameters of open cells observed are used for numerical spectral wave modeling by superimposing the gusts into conventional coarse input wind field (results of an atmospheric model). The results confirm that a moving "open cell" causes the local significant wave height increase in order of meters within the cell area and especially in a narrow area of about 2.5km at the footprint center of a cell. A group of cells for real storm condition produces a local increase of significant wave height of more than 6m during a short time window of 10min-20min (passing the cell). Wave groups including extreme individual waves with wavelength of more than 370m under the cell's footprint are estimated. This corresponds well with measurement of a rogue wave group with length of about 400m registered during storm "Britta" and damaged the deck of research platform FiNO-1 in 18m above Mean Sea Level in 2006.

Such events on a smaller local scale, where the local wave height increases by 1-2m in kilometer-size clusters is accompanied by wind gusts in the German Bight can be now observed and investigated using new techniques based on satellite-borne SAR data.

Over the last years, a number of new high resolution X-band radar satellites have been launched which provide the possibility to image and measure the sea surface with high resolution, e.g. TerraSAR-X (TS-X), TanDEM-X (TD-X) and COSMO-Skymed satellites. This opens a new perspective for investigating sea state and connected processes in coastal areas, where spatial variability plays an important role. A wide spectrum of features and signatures at the sea surface are simultaneously involved and can be observed in high resolution images including surface wind and gusts, individual waves and their refraction, wave breaking effects, etc. Knowledge of basic geophysical processes and their imaging mechanisms is necessary for the successful processing of images and for organizing NRT services to provide the information to interested users like national meteorological services.

1.2. Sea State in SAR imagery

Ocean surface measurements by SAR have been done since the first space borne SAR missions in 1971. This includes such well-known missions as L-band SAR SEASAT launched in 1978, C-Band European Radar Satellites ERS-1 and ERS-2 launched in 1991 and 1995, ENVISAT (Environmental Satellite) with C-Band Advanced Synthetic Aperture Radar (ASAR) in 2002 and other. The extraction of surface ocean waves and wind parameters received priority in a number of other tasks. In fact, in the case of surface waves, the radar return echo is dominated by Bragg scattering of short ripple capillary waves of the order of centimeters, produced by wind at the sea surface. A SAR image exhibits the ability of the sea surface to reflect the radar signal: surface roughness produced by waves on all scales from small capillary waves to large ocean surface swell waves. As moving and unstable targets, the waves are often deformed, defocused and smoothed the SAR images. Conventionally, the SAR imaging mechanism of the sea surface created by waves as described in literature (e.g. Hasselmann el al., 1985) is based on the Real Aperture Radar (RAR) mechanism with additional specifics connected to SAR. The classic approach is the estimation of the image spectrum from a subscene and converting this spectrum into a wave spectrum using a transfer function under a series of assumptions.

The first generation original inversion method of Hasselmann and Hasselmann (1991) was based on a maximum likelihood matching of the first guess (prior) information available from a wave model and the data provided by the SAR wave image spectrum. From the first-guess wave spectrum, the forward transform is applied to first compute the associated SAR wave image spectrum. It is undisputed that second-generation retrievals, which use the complex information of the image cross spectra to remove the directional propagation ambiguity, are inherently superior to first generation retrievals using only SAR image variance spectra (Li et al., 2010).

An empirical algorithms were considered to retrieve integral wave parameters for C-band SAR data (Schulz-Stellenfleth et al., 2007) which were used for the ERS missions. This approach was further extended for using for SAR data acquired by the ENVISAT (Li et al., 2008) without using *a priori* information. Nevertheless, approaches of both generations engaged only in the study of waves and disregard the wind information. However, in geophysical natural processes wherein the waves are strongly connected to the local wind, such cross information can significantly improve performance.

1. 3. TerraSAR-X and TanDEM-X for maritime parameter estimation

The X-band SAR satellite TS-X (launched in 2007) and its twin TD-X (launched in 2009) operate from 514km height at a sun-synchronous orbit with a ground speed of 7km · s^{-1} (15orbits per day). They operate with a wavelength of 31mm and a frequency of 9.6GHz (Breit et al., 2010). The repeat-cycle is 11 days, but the same region can be imaged by different incidence angles after three days dependent on scene latitude. Typical TS-X incidence angles θ range between 20° and 55°. From the point of sea state SAR processing, a larger incidence results in stronger non-linear effects from the focusing of moving wave crests. This is caused by an increase of the acquisition distance (slant range Ro) by a factor of about two: Ro =546km for θ=20° and Ro=896km for θ=55°. For example, the Doppler-shift (displacement in azimuth direction y,) of a target moving with radial velocity u_r=1m·s^{-1} towards the sensor flying with a platform velocity V_{SAR} (7km·s^{-1} for TS-X) at slant range R_o distance $D_y=(ur/V_{SAR})\cdot R_o$ (Lyzenga et al., 1985) and results in ~70m for incidence angle of 22°. It is reduced by a factor of about two for TS-X (~120m for ENVISAT ASAR for the same incidence angle) in comparison with earlier SAR missions due to the lower TS-X altitude.

The TS-X data used for the study are Multi-Look Ground Range Detected (MGD) standard products with pixel spacing of 1.25m for StripMap mode (resolution of 3m). Figure1 demonstrates an example for the processing of meteo-marine parameters from a scene acquired over the German Bight in the North Sea by the TerraSAR-X (TS-X) radar satellite. For processing of the scene the latest developed Sea State Processor (SSP) based on empirical model functions XWAVE_C (C=coastal, sea state) and XMOD-2 (Li and Lehner, 2013) (wind speed) designed for NRT services from TS-X X–band data are used and explained in following sections.

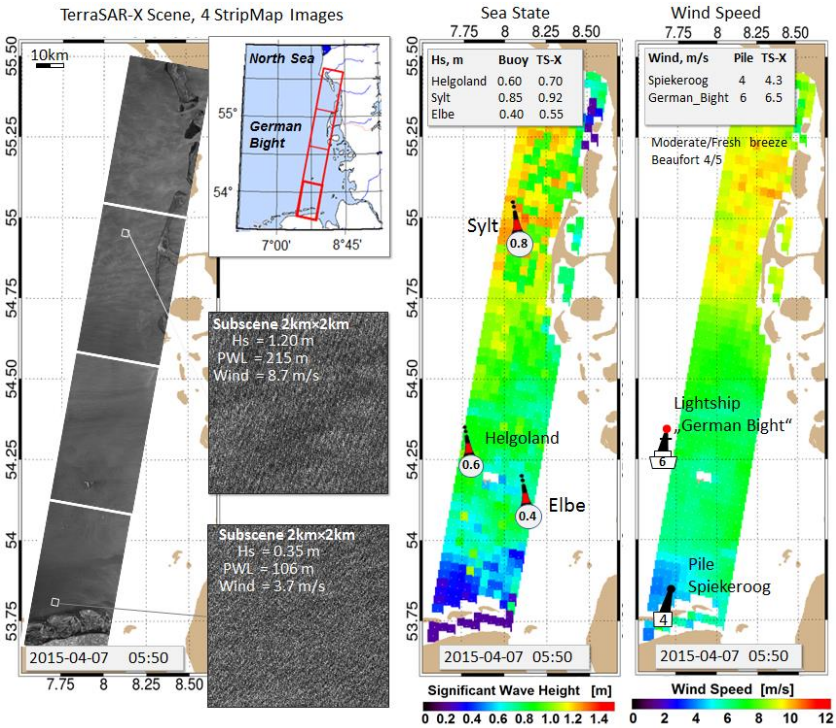

Fig.1: Meteo-marine parameters (Total Significant Wave Height H_S and surface wind speed U_{10}) processed with 3km×3km posting using a newly developed Sea State Processor with empirical XWAVE_C (Coastal) algorithm from TerraSAR-X StripMap scene acquired over the German Bight of the North Sea on 07.04.2015. Local wind speed is estimated using the XMOD-2 algorithm for the same subscenes analyzed. The wind is about 4-6m · s^{-1} (moderate breeze, Beaufort 4) in the south part of the Bight and intensifies in the North to 10-11m · s^{-1} (fresh breeze, Beaufort 5). The collocated measurements represent the H_S in meter for wave rider buoys and the wind speed U_{10} in m · s^{-1} for lightships and piles (right) are also shown.

Fig.2: Air photo taken on 29.09.2013 by Ralf Roletschekek over the North Frisian Wadden Sea with island Trischen in the foreground. In ~10km background the German coast is visible (Büsum). Wadden Sea is characterized by a strong dependence on tides in complex topography with a large number of islands and shoals. The tidal changes of water levels can reach several meters and corresponding variations of the local currents are more than $2m \cdot s^{-1}$ during few hours. Numerous sandbars and shoals appearing during low water tide greatly influences the spatial distribution of the wave propagation.

1. 4. Sea state in intertidal zones of the North Sea

The German Bight in the North Sea includes a part of the Wadden Sea and is characterized by a strong dependence on tides in complex topography with a large number of islands and shoals. The tidal changes of water levels can reach several meters and corresponding variations of the local currents are more than $2m \cdot s^{-1}$. Numerous sandbars and shoals appearing during low water tide greatly influences the spatial distribution of the wave propagation.

The wave models of the third generation have been developed and used for sea state prediction, e.g. the WAM model (WAve Model) used by forecast services in Europe like ECMWF (European Center of Medium range Weather Forecast), the German Weather Service (DWD, http://www.dwd.de), and the Danish Meteorological Institute (DMI, www.dmi.dk), which are a part of the global marine weather and warning systems. In the open sea (deep water) the wave models are already capable to produce a high-quality forecasting service (Behrens and Günther, 2008) as long as the wind input from atmospheric forecast models and the boundary conditions are correct.

The uncertainties are present when dealing with numerical modelling in coastal areas: the physical processes in shallow water, caused by the interaction between waves, currents and the sea bottom become important. The spatial wave properties are changing strongly in coastal areas. The variable depth in shallow areas results in depth-forced changing of wave length and wave height. The shortening of the wavelength is compensated by wave height increase (shoaling effect). Due to bottom influence the wave energy is dissipated and transferred into turbulence and acceleration of flow currents (radiation stress). As a result, the current structure will undergo a significant change at the coast and around the sandbanks, where dissipation is the strongest. In the German Bight a long-shore current of some $30\text{-}50cm \cdot s^{-1}$ of magnitude appears in the near-shore zone approximately 0.5km wide. Local variations exceed $2m \cdot s^{-1}$ if waves are completely dissipated due to large localized topographic gradients under storm conditions. Large areas like the Hörnum-Bight gain an increased

sea level (Pleskachevsky et al. 2009). The waves are reacting to the increased water depths and higher sea state occurs.

The intensive transport shipping and unloading at offshore construction sites like wind parks in the German Bight requires an improving of forecast accuracy. For a ship docking on an offshore construction a wave height <1.3m is required. The users (e.g. shipping companies) had requested an improvement of sea state prediction in the significant wave height H_S in range of 0.5m-2m. In case H_S exceeds 1.2m, the disembarking is too hazardous for crew members and the transport ship must return back to the harbor. Such works are planned in advance and inaccurate predictions cause high additional costs.

1.5. New Coastal Wave Model CWAM by German Weather Service DWD

The high resolution Coastal Wave Model (CWAM) for the German Bight and the western Baltic Sea has been developed by DWD and BSH in cooperation with the Helmholtz-Zentrum Geesthacht (HZG). CWAM is based on the Wave Model (WAM) and will complement the series of wave models consisting of the Global Wave Model (GWAM) and the European Wave Model (EWAM) which are operated by the DWD. The wave CWAM model was coupled to the circulation model of the BSH which uses the same bathymetry grid. The purpose of this modification was to improve the forecast quality especially near the coast, where the bathymetry varies greatly in space and currents and water level vary temporally. CWAM runs in a pre-operational state for an extended forecast time range of 48 or 72 hours (Kieser et al., 2013). Local differences of resulting H_S EWAM/CWAM in coastal areas are in the range of meters because of more structure in bathymetry (1) and rapid change of water level and circulation currents by tides (2) (see Fig.3).

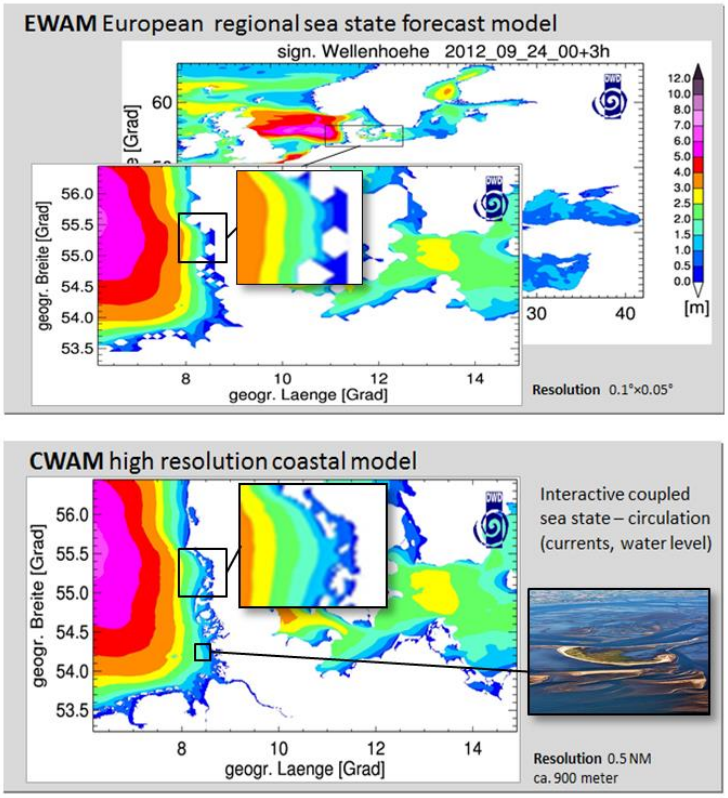

Fig.3: Conventional EWAM sea state forecast and new high resolution coastal model CWAM (0.5NM=~900m). Local differences of resulting H_S in coastal areas are in the range of meters because of more structures in bathymetry (1) and rapid change of water level and circulation currents by tides not resolved by EWAM in intertidal Watt zone (2).

Figure 4 shows the new DWD CWAM bathymetry in the German Bight and collocated 6 buoys. A subscene from TS-X Stripmap image around Trischen Island demonstrates that despite the very detailed 900m bathymetry, the real conditions are even more complex. This is necessarily reflected in the propagation and distribution of real waves. The red lines in the TS-X image are created by an automated waterline detection algorithm for the Wadden Sea, a new development also to be implemented into the NRT processing chain (Wiehle and Lehner, 2015; Wiehle et al., 2015).

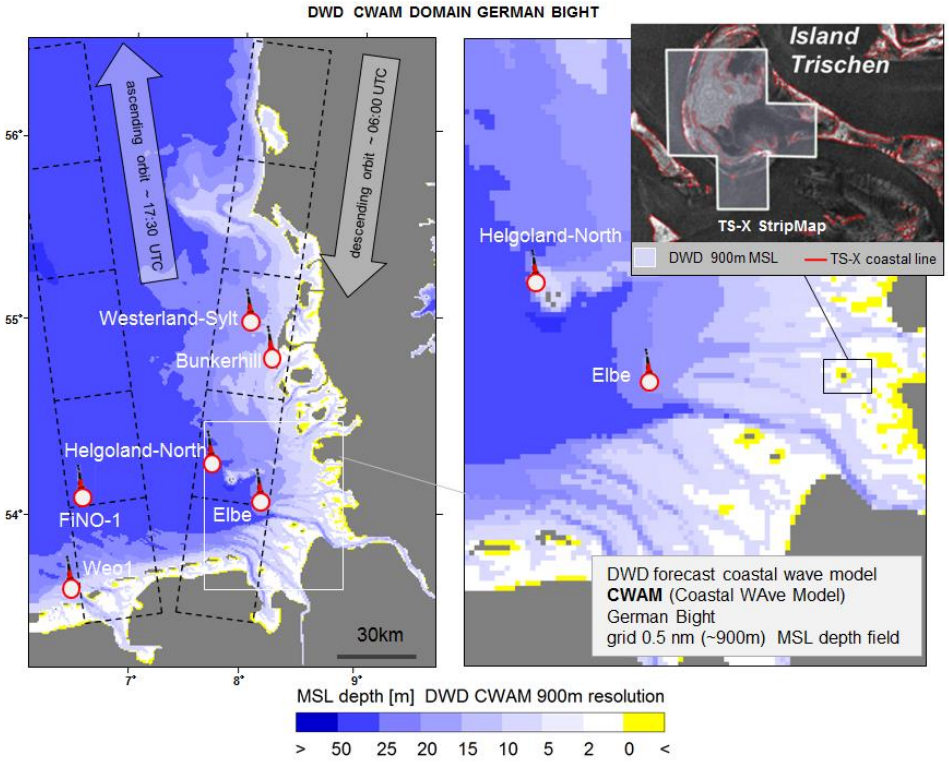

Fig.4: DWD CWAM wave model domain in the German Bight with 0.5 nautical mile (~900m) horizontal resolution. The Wadden Sea area is well pronounced by a series of islands, sandbars, ridges, inlets and shoals. A subscene from TerraSAR-X Stripmap image around Trischen island demonstrates that despite the very detailed 900m bathymetry, the real conditions are even more complex. This is necessarily reflected in the propagation and distribution of real waves (right). The concept for TerraSAR-X scene ordering in the German Bight is shown: two typical ascending and descending overflights collocated with 6 available buoys; each scene consists of 3-6 StripMap images.

2. Sea State estimation from TerraSAR-X images

2.1. XWAVE_C for coastal applications in Wadden Sea

It is known from statistics that the wave height in range of 0-2m in the German Bight is presented mostly by local short windsea with wavelengths <120m. These waves are often well spread in frequency and direction and do not represent ordered long wave crests like swell. In SAR imaging such waves are either invisible (wavelength L<~50m), producing image noise, or barely visible (~50<L<~100), producing non-linear distortions in form of defocusing streaks. The contribution of such "unstructured" waves for total significant wave height is in the order of 0-1.5m and is usually neglected for global ocean applications where the long swell waves are investigated. For coastal application, namely these short-crest waves, their contribution and their SAR imaging are investigated and considered in the model function in order to reach the required accuracy.

The development of a tool to estimate meteo-marine parameters from satellite-borne SAR data allowing strictly to distinguish the waves in the H_S range of 0m-2m with decimeter accuracy for highly variable coastal environments included three tasks:

(1) Designing an empirical algorithm-function XWAVE_C (C=coastal) based on earlier studies (Bruck, 2015, Lehner et al., 2013), using the approach of a direct estimation of integrated sea state parameters from SAR image spectra without transformation into wave spectra. The further development of this proven approach was chosen because of the need for robust rapid data processing not giving the time for sophisticated and long mathematical iterations for the transformation. As the model-function estimates the wave height correctly only in case the scene analyzed includes the "pure" sea state only, a series of filtering procedures should be developed and included before and after the function is applied to remove the artefacts like ships, seamarks, etc. from the scenes and to correct the results.

(2) Integrating the XWAVE_C model function, wind estimation algorithms, filtering and checking procedures into a Sea State Processor (SSP). The SSP is installed in the NRT processing chain at the satellite ground station "Neustrelitz". It includes also a parameter-based user interface and sequently performs stable raster analysis of multiple TS-X images.

(3) Ordering, collecting and processing the data; analysis of results, verifications.

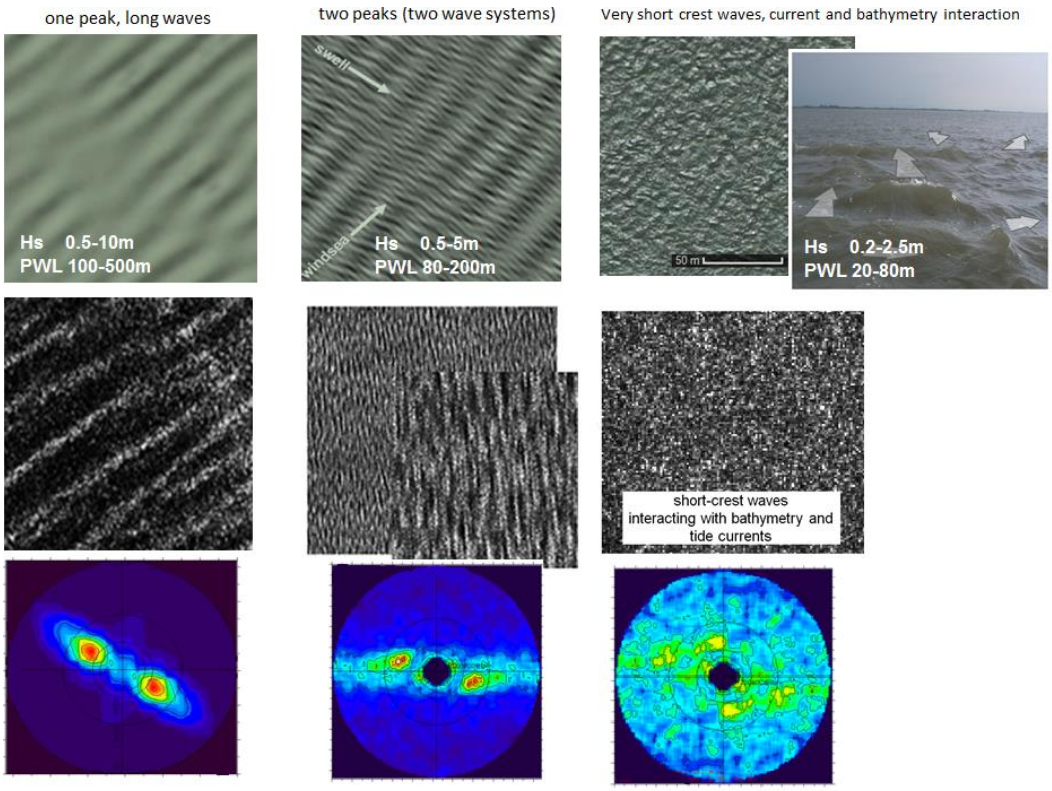

Fig.5: Schema for different sea sates imaging by TerraSAR-X (first row - random surface simulation from wave spectra and a cut form Google Earth image over German Bight). Well imaged long swell waves (low wind), the shape of image spectra approaching the form of wave spectra, near linear imaging (left). Windsea by strong wind covers the long waves by amount of short-crest waves: defocusing structures from short and fast moving and deforming targets covers imaging of swell (middle) and typical low sea state in coastal areas of German Bight (right): the short waves interact with strong tidal currents and the bathymetry while running on numerous sandbanks and shoals. The very short wave crests present a large number of small, nonstable and fast and chaotically moving targets for SAR sensor. Such a sea state in domain H_S 0-1.5m is typically imaged as a noise with a hardly recognized wave pattern with noise properties connected to wave crest amplitude and speed.

An empirical XWAVE_C model function for obtaining integrated wave parameters has been developed for X-band data as XWAVE-2 (Bruck and Lehner, 2013; Bruck, 2015) for deep water firstly. XWAVE-2 was based on the analysis of image spectra and uses parameters fitted with collocated buoy data and information on spectral peak direction and incidence angle.
The main parameter is the integrated value of the directional wave number Image Spectrum (*IS*) E_{IS}.

$$E_{IS} = \int_{k_x^{min}}^{k_x^{max}} \int_{k_y^{min}}^{k_y^{max}} IS(k_x, k_y) dk_y dk_x \qquad (1)$$

where Image Power Spectrum in wavenumber $IS(k_x,k_y)$ (y=satellite flight direction, x=to-satellite direction) with $k^{MAX}=\pi/$(subscene_size) domain is obtained by using FFT (Fast Fourier Transformation) on a subscene of the radiometrically calibrated TS-X/TD-X intensity image. The integration domain is limited by the maximal wavelength L_{max}=600m corresponds to k_{min}=0.01 in order to avoid the effects of wind streaks signal produced by turbulent boundary layers (1) and by minimal wavelength L_{min}=30m correspond to k_{max}=0.2 to avoid SAR image distortions from short sea surface waves and wave breaking streaks entering the domain 0-30m (2).

The XWAVE-2 algorithm was tuned primarily using data acquired over NOAA buoys in open oceans worldwide and in the northern part of the North Sea where measurements near oil platforms (e.g. EKOFISK) are available. XWAVE-2 was capable to estimate integrated wave parameters with Scatter Index $SI_{Hs}^{XWAVE/BUOY}$=21% for waves in the range about 2m-15m wave height with a mean value of 3.6m and $SI_{L}^{XWAVE/BUOY}$=13% for wavelengths in the range 80m-600m with a mean value of 240m (Bruck 2015). These results are more than satisfactory for open seas and for a global analysis.

The XWAVE-2 algorithm works well in open ocean waters and was successfully tested also in coastal waters near oceanic islands like the Canarias Islands (Bruck et al., 2011) and Rottenest Island near Australia. However, even the first tests of XWAVE-2 in the shallow waters of the German Bight highlighted the need for significant improvements. In fact, the sea state in front of the oceanic islands' coasts is dominated by long waves propagating in sufficient depths and refracting around the like table-mountain islands with steep coasts: the sea state conditions are similar to the sea state conditions used for algorithm tuning. Applied for short and steep sea state in the German Bight, the algorithm results in strong overestimation of wave height by a series of signals unknown to the algorithm (moderate conditions with H_S in range 0.2-3m). On the other hand, during storms while the long waves with wavelength >200m dominate, XWAVE-2 matches the measurements in selected subscenes in the German Bight.

The XWAVE approach has been repeatedly validated and adopted for coastal sea state in order to check and modify the performance by cross impact analysis. The first guess $Hs^{XWAVE-2}$ from XWAVE-2 was applied to study and determine sources for perturbations and outliers. The connections of errors with spectral parameters have been established and explained.

TS-X scenes were pre-processed and the spectral parameters estimated by scene analysis were collected. The parameters which turned out to be the most important were: U_{10} - local wind speed using XMOD-2 (Li and Lehner 2013) algorithms; the ratio $R^{in/out}=N_S{}^{in}/N_S{}^{out}$ that indicates the character of non-linearity of the imaging mechanism and the ratio $R_E{}^{30/E400}=E^{30}/E^{400}$ indicates the relation of energy from real long waves (80m-400m) to noise energy produced by streak-structures (30m-80m) in case of appearing non-linear effects (the local wind speed U_{10} helps to separate them from local short windsea). An explanation for $R^{in/out}$ see in Fig.6 where example for three TerraSAR-

X acquisitions for similar sea state traveling in different directions (peak wavelength PWL ~70m-100m) are shown.

E^{30} integrated energy of a spectrum annulus corresponds to wavelength 30m-80m.
E^{400} integrated energy of a spectrum annulus corresponds to wavelength 80m-400m.
N_S^{in} spectrum noise inside of so-called "*cut-off*" domain of the spectrum.
N_S^{out} spectrum noise outside of so-called "*cut-off*" domain of the spectrum.

The developed XWAVE_C function for coastal application is presented by equation:

$$Hs^{XWAVE\_C} = a_1\sqrt{B_1 E_{IS}\tan(\theta)} + a_2 B_2 + a_3 B_3 + a_4 B_4 + a_5 B_5 \qquad (2)$$

where a_1-a_5 are coefficients (constants) and B_1-B_5 are functions of spectral parameters. The first two terms introduce positive contributions in wave height and the last three are negative deductions for eliminating outliers of different kinds. B_1 represents noise scaling of the total energy E_{IS} (short wind waves and their breakings produce an additional noise that influences resulting energy, $B_1=x_0R^{in/out}$ with x_0 tuned using collocated buoy data). The second term a_2B_2 represents wind impact with $B_2=U_{10}$. However, a_2 is found to be not a unique constant; for strong wind $U_{10}>19\text{m}\cdot\text{s}^{-1}$ a_2 is modified to express the transition of wave regime into strong breaking and flying water particle targets (Beaufort 9). The terms a_3B_3 and a_4B_4 are corrections for eliminating the impact of short (e.g. wave breaking induced) and long (e.g. wind streaks) structures in the SAR image, respectively. These structures result in spectral peaks and diffused spectra energy not directly connected to the sea state: $B_3=R^{E30/E400}$ and $B_4=E^{600}$. The last term a_5B_5 with $B_5=E_K$ is a correction for outliers produced by extra-large structures like sandbanks or ship wakes which have not been pre-filtered.

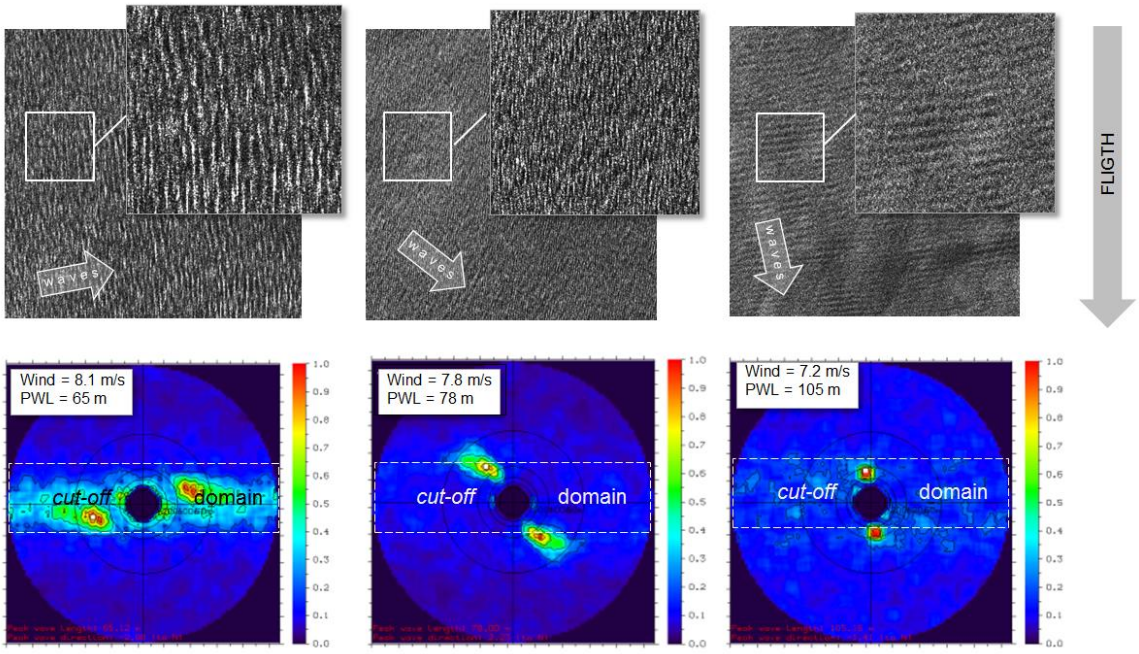

Fig.6: Example for three TerraSAR-X acquisitions for similar sea state traveling in different directions (peak wavelength PWL ~70m-100m): azimuth traveling (right), range traveling (left) and intermediate situation. The wind speed is ~7-8m · s-1for all subscenes. The near-azimuth traveling waves are minimally distorted by non-linear effects (ratio $R^{in/out}$ ~1), the shape of image spectra approaches shape of wave spectra; for 45° traveling waves the non-linear distortions are already visible (ratio $R^{in/out}$ ~2), and for range traveling waves, the distortions dominate (ratio $R^{in/out}$ ~4).

Initially, the algorithm was intended for VV polarization. However, the users of NRT services order often HH polarisation that is more convenient for tasks like ship detection. Therefore, an adoption for HH polarization was also incorporated.

The sea state estimated for U_{10} <2m · s^{-1} is classified as not reliable. In general, visible capillary ripples responsible for radar return echo are developed under surface wind speeds >2-3m · s^{-1}. Thus, the signal with local wind speed less than U_{10}^{min} =2m · s^{-1} can be interpreted as clatter.

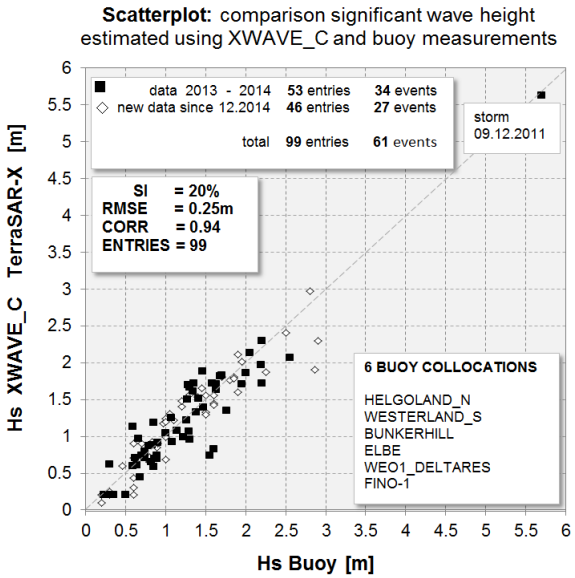

Fig.7: Total comparison of all available data acquired over the German Bight in 2013-2015 including a storm on 09.12.2011: 61 TerraSAR-X Scenes (overflights/events/days) with 201 StripMap images and 99 buoy collocations (collocation around 30min and up to 5km spatially).

TS-X scenes were processed with 3km×3km posting (~10×15=~150 subscenes per image). The collocations were done with a time window of +/- 10min for comparison with model data and +/- 20min for buoys (slightly varying recording period). CWAM hourly output is at 6:00 and 18:00 UTC and acquisition time for TS-X is 05:50-06:10 for descending orbit and 17:50-18:10 for ascending orbit in German Bight. Spatial collocation occurred in a domain up to 5km. A source of uncertainties for comparison lies in the fact that a buoy represents statistics of a small sector of sea state propagating towards the buoy, integrated over time (typically 20min time series). TS-X represents HS from statistics of a wider "frozen" area (snap shot) which includes more variability than buoy data due to e.g. bathymetry disturbing the homogeneity of sea state. As a result, HSbuoy and HSTSX are the same only in case no temporal (~20min) and no spatial variations (~5km×5km) occur in sea state statistics.

The local comparison of the TS-X estimated wave height with *in-situ* buoy measurements was conducted for 6 stations in the German Bight (Fig.4). The scatter index SI$^{TSX/BUOY}$=20% was obtained for all data (for tuning data until 12.2014 and as well for residual data verification, see Fig.7). The statistical analysis shows the averaged value of collocated H_S to be about 1.5m in the German Bight at buoy locations (no buoys are located beyond 50km from the mainland in deep water). Acquisitions with H_S>2.5m occurred quite rarely. It was only once managed to acquire a storm condition with H_S>3m (09.12.2011) in the German Bight near the coast (descending orbit) and four times in open sea over ALPHA VENTUS offshore wind park (10.12.2014, 21.12.2014, 01.01.2015, 12.01.2015).

2.2. Artefact interfering sea state estimation and their filtering

A direct implementation of the Empirical Model Function (EMF) Eq.1 in coastal areas even for storm conditions leads to more than 50% errors of processed data with outliers in the range of meters for H_S. The sources of error are in the first place a number of natural and man-made artefacts typical for Wadden/mudflat coastal waters: sand banks, wave breaking, ships, current boundaries and also atmospheric fronts. Even internal wave structures impact the image spectra. Such spectral perturbations result in an integrated value which yields a contribution to the total energy that is not connected to the sea state. Figure 8 demonstrates the impact of different artefacts (ships and wind parks) on the resulting image spectra; the "pure" sea state and its spectra are also shown for comparison. Even the shape of such spectra differs principally from wave-produced spectra shapes; the produced spectral energy is not connected to the sea state and reaches values several times higher than the surrounding signal from the waves.

In order to exclude errors from ships, buoys and other artefact signals, a pre-filtering procedure has been adopted before the FFT analysis and the wind estimation for each analyzed subscene. After the statistics for a subscene is estimated, the subscene is analyzed using a 150m×150m sliding window (sub-subscene). The sub-subscene statistics is compared with the statistics of the subscene and outliers in the sub-subscene are replaced by the mean value of the subscene.

Generally, in StripMap TS-X images acquired over the open ocean, spatial changes of the sea state are not well pronounced for long waves. Consequently, even if an image is "spoiled" by artefacts like oil, organic spots or ships, the concept was to select the subscenes admitted for analysis using a continuity check. In coastal areas, where it is difficult to find a location without artefacts like ships, buoys, sandbars etc., the procedure of artefact pre-filtering and result control is absolute necessary for raster sea state analysis.

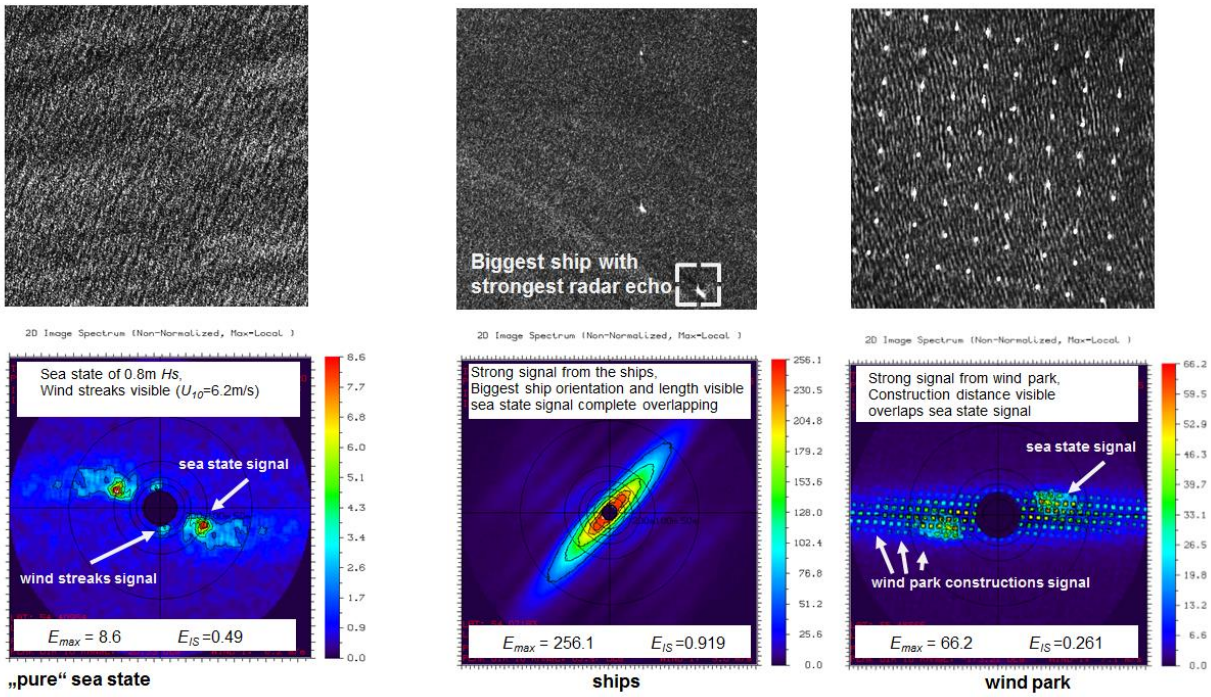

Fig.8: Artefacts for sea state estimation in TerraSAR-X subscenes (top) and corresponding image spectra (bottom): ships (left) and wind park (middle). The "pure" sea state suitable for conventional estimations is shown for comparison (left).

3. Sea State Processor for NRT services

3.1. Sea state processor for practical use

All operations described before are integrated into the Sea State Processor (SSP) developed for both HH and VV polarisation. The SSP is developed in C++ code and performs the following steps:

- Step-1: reading and calibrating the SAR image, reading User Control parameters and GMF parameters,
- Step-2: selection of a subscene and pre-filtering (removing image intensity artefacts like ships, buoys etc. based on local intensity statistics),
- Step-3: calculation of XMOD-2 wind,
- Step-4: spectral analysis of the subscene (FFT, integration and spectral parameters),
- Step-5: wave height estimation using XWAVE_C GMF (SSP core),
- Step-6: checking of results using wind speed and integrated spectral parameters (e.g. long structures like sand banks produce high spectral values in domain k<0.01 and can be separated) and generating outputs.

The SSP includes also three control units to operate the processing (e.g. FFT size, raster analysis step, settings of ship filtering, image spectra integrating, etc., for a total of 41 parameters), outputs (results, statistics) and settings of the model functions. The SSP was installed at the Ground Station "Neustrelitz" (Pleskachevsky et al., 2015, Schwarz et al., 2015) to provide an operational service and has been tested. The delivery of NRT products from "Neustrelitz" to the user (e.g. DWD) occurs by E-mail and by FTP transfer. For the common users, a file with the data (lon, lat, H_S), the Google Earth file (.kmz) to preview the image file (.jpg) with color-coded wave heights are provided.

For example, a TS-X StripMap acquired over the German Bight on 15.07.2015 at 05:51 UTC was NRT processed in the ground station "Neustrelitz" using the installed SSP. At 07:04 UTC, the results (file includes geo-coordinates with H_S values) had been transferred to DWD and automatically overlaid on their CWAM forecast wave height map of 06:00 UTC. This validation shows the local variation and differences in sea state in comparison to predictions, e.g. a long Scharhörnplate-sandbar near Scharhörn-island was partially dry (no waves) while in the model prediction the bar was wet with H_S~0.5m.

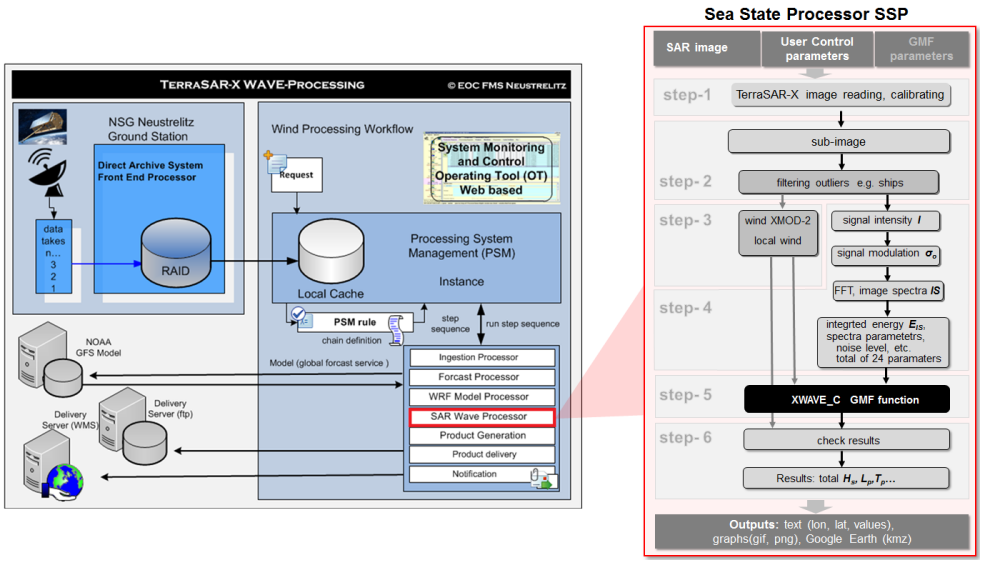

Fig.9: NRT-processing chain for TerraSAR-X data in DLR ground station Neustrelitz. The Sea State Processor was integrated into the chain (marked in red).

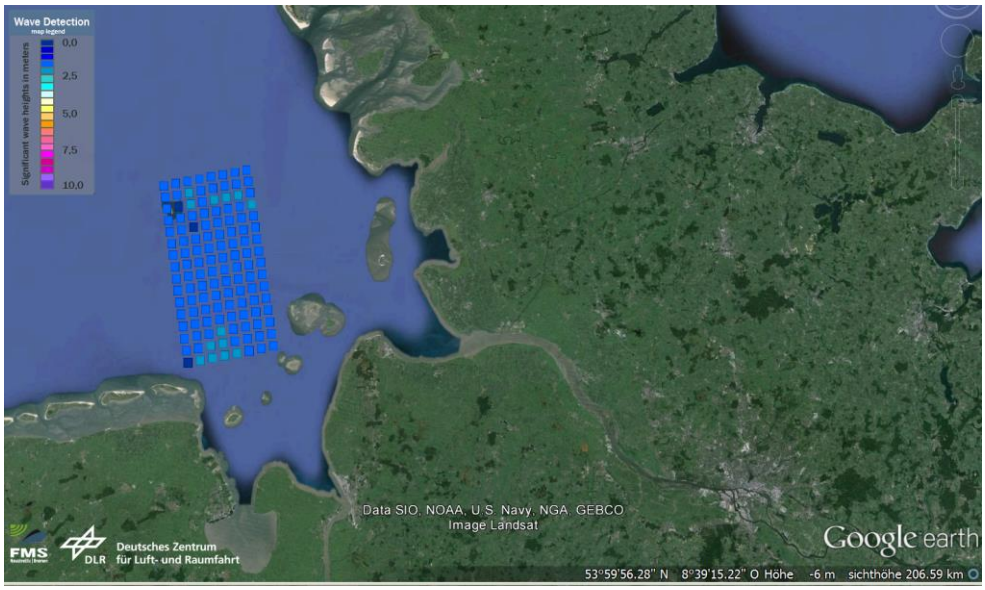

Fig.10: NRT-processing example for TerraSAR-X acquired on 22.11.2015 at 17:10 UTC over German Bight. For the common users, a file with the data (lon, lat, H_S), the Google Earth file (.kmz) to preview the image file (.jpg) with color-coded wave heights are provided.

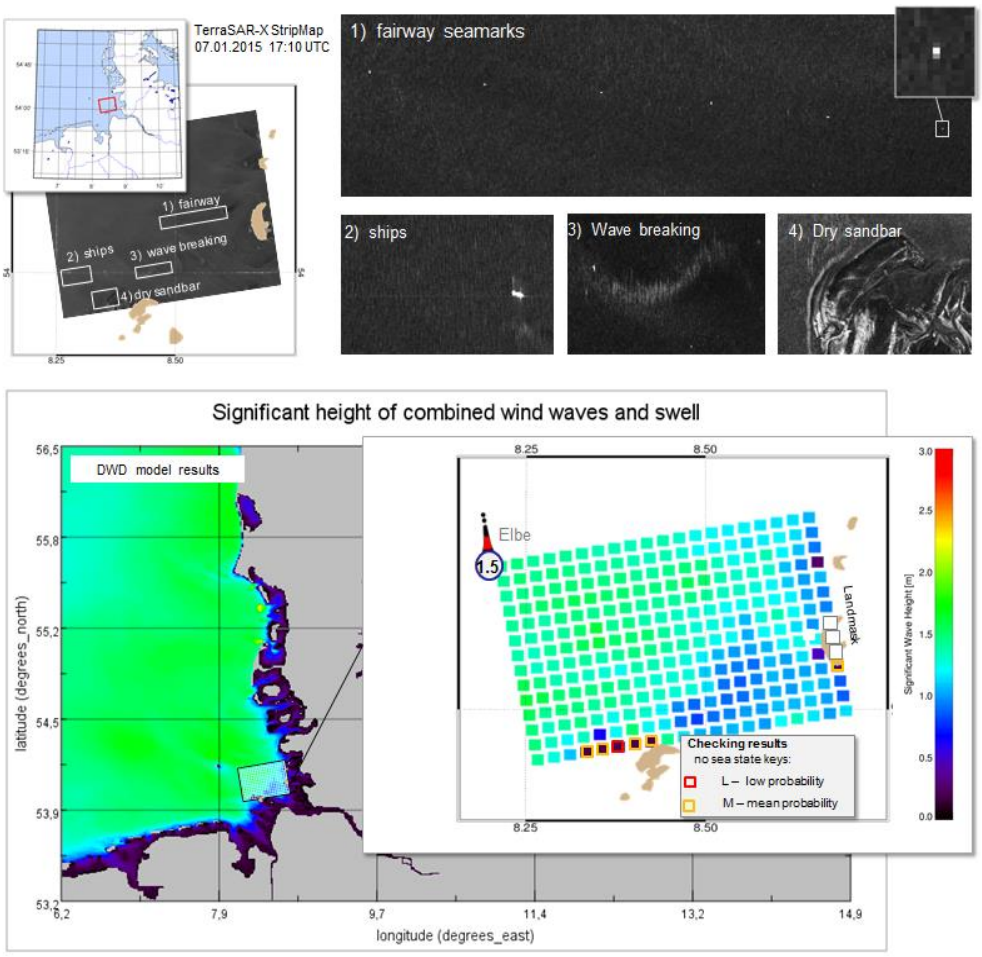

Fig.11: Example for the performance of the Sea State Processor using the XWAVE_C function. The analyzed scene acquired on 07.01.2015 over the German Bight includes SAR structures produced by sea state and by other features: ships, dry sandbars, buoys and seamarks (bottom left). A pre-filtering of artefacts before FFT analysis and corrections for large structures with high energy in k-domain and an additional checking based on statistics of the integrated energy of the whole scene improve the estimated results (bottom) overplayed over DWD model results.

3.2. Sea State Processor: control of results

It is impossible to filter out all the errors in analyzed subscenes immediately, while the statistics over the whole scene is not computed. After the whole scene is processed, the statistics of E_K (Spectral energy integrated with dividing each spectral k-bin by k^2, amplifying high frequency spectrum signals, e.g. ships, long edges, etc.) is used to check the results. An exceeding of mean value $\overline{E_K}$ for non-land points and for points with local wind $U_{10}>U_{10}^{min}$ by $E_K > q \cdot \overline{E_K}$ with matched q ensures isolating of no-sea-state subscenes like dry sand bars and wave breaking locations. The output values were assigned with keys:

(1) "H" for High probability (99%) sea state,
(2) "M" for Medium probability (50%) sea state: sea state might be altered by artefacts e.g. sandbars;
(3) "L" for- Low probability sea state: no sea state;
(4) "N" – No wind available: the local wind$<2\text{m} \cdot \text{s}^{-1}$, the results are not trustworthy and
(5) "I" – Island or Land: more than 10% of the subscene analyzed is mainland (land mask).

The SSP interface allows the user to change the pre-installed properties of automatic data processing and output (e.g. posting step, initial setting: 3km). The output writing of four text-file types is possible with additional graphic view as TIFF files for processed image, sub-scenes, 2-D and 1-D spectra (optional) are possible:

(1) TSX_acquisition-date_mean-values.txt contains the mean values of all parameters for the scene (H_S, wind, intensity, incidence angles, geo-coordinates, spectral parameters, etc.);
(2) TSX_acquisition-date_waves.txt contains only geo-coordinates and H_S estimated (for extern users);
(3) TSX_acquisition-date_results.txt - all parameters such as scene size, resolution, polarisation, integrated energy, noise and other details for each analyzed subscene are stored.
(4) TSX_acquisition-date_special-points.txt contains information for minimal distance of subscenes analyzed to special points (e.g. buoys and offshore construction) specified in input file spetial-points_input.txt (for the German Bight, 6 spatial points were used: measurement piles, wave rider buoys).

4. Results and validation examples

An example for processing of a TS-X scene acquired on 07.01.2015 over German Bight is shown in **Fig.11**. The image includes SAR signals produced by sea state and by other features: ships, dry sandbars, buoys and seamarks (bottom left). A pre-filtering of artefacts before FFT analysis and corrections for large structures with high energy in k-domain and an additional checking based on statistics of the integrated energy of the whole scene improve the estimated results (bottom).

The sequences of TS-X StripMap images (scenes) cover streaks of 300km×30km across the German Bight and allow observing the local variation in wind and wave fields. Figure 12 shows an example of covering different weather conditions by the same TS-X orbit. For wind speed$<2\text{m} \cdot \text{s}^{-1}$ HS values were masked out (unconfident) with local wind speed estimated using the XMOD-2 algorithm.

Already the first validations revealed that TerraSAR-X data show a more complex structure than CWAM data (Kieser et al., 2013). During algorithm validation and verification, a number of TS-X images acquired over German Bight were collected. These data allow a first assessment of the spatial distribution of meteo-marine parameters and their relationships on a local scale. The data cover large

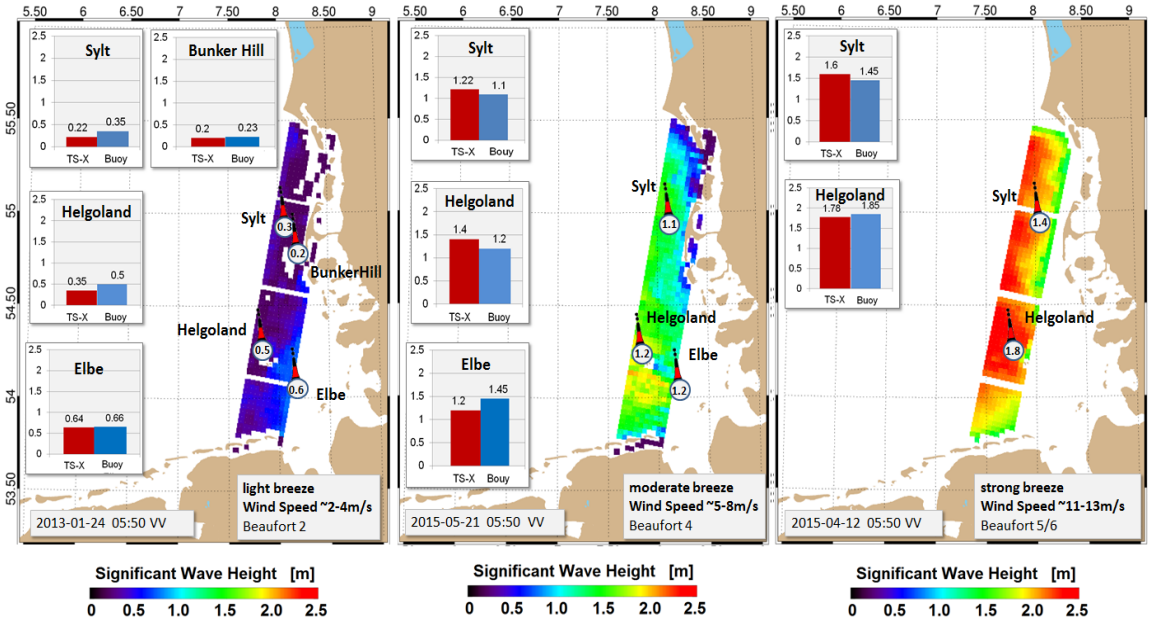

Fig.12: Example of the sea state at different weather conditions: (Total Significant Wave Height H_S) over the German Bight estimated with 3km×3km posting using the Sea State Processor with an empirical XWAVE_C algorithm on TerraSAR-X StripMap images. Three different weather conditions and comparisons to buoy measurements are shown. For wind speed<2m $\cdot$ s^{-1} HS values were masked out (unconfident) with local wind speed estimated using the XMOD-2 algorithm.

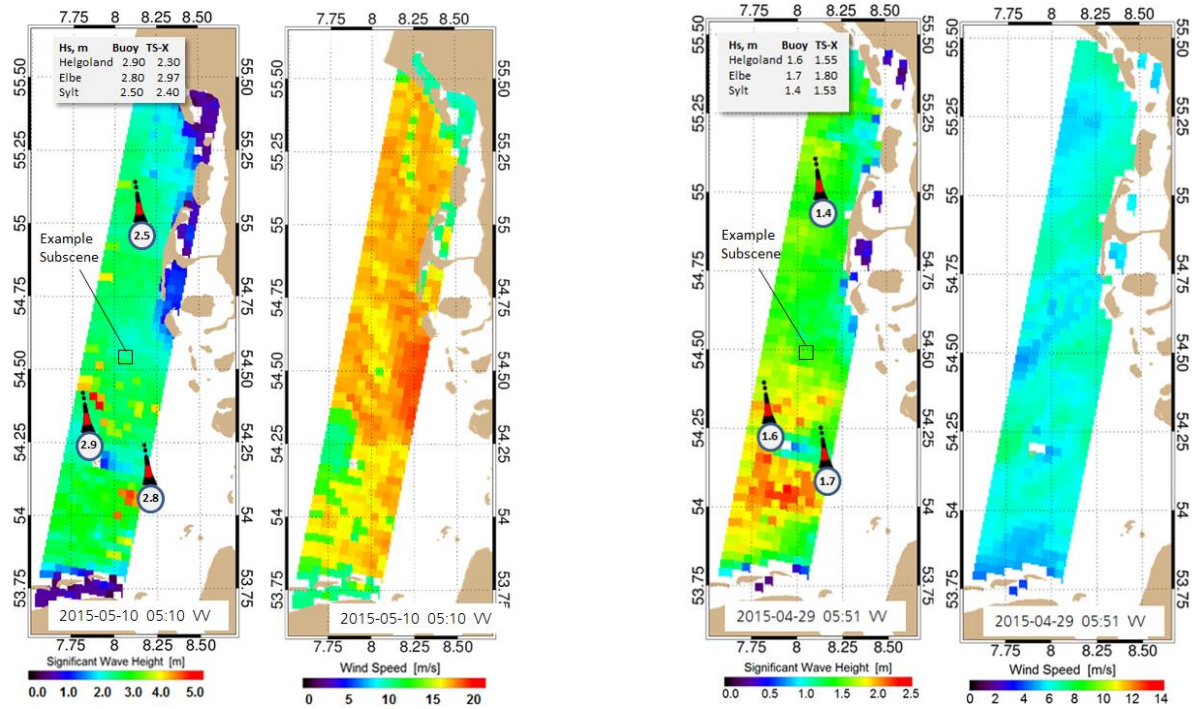

Fig.13: Examples of waves and wind derived with SSP (XWAVE_C) and XMOD-2 model functions for the German Bight: on 05.10.2015 and on 04.29.2015. Both overflights are identical, but show different wind and sea state conditions: stormy wind with gusts, the wind gusts produce a local increase of significant wave height (left) and moderate wind (right).

spectra of weather conditions and sea state system combinations. Although the storm acquisitions are rare, a number of scenes for sea state in the wave height domain 0.2-5m (value of HS ~1.3m is important for a safe ship docking at offshore constructions) give a new possibility to detailed investigations of local sea state inhomogeneity and front shifting in comparison to forecast models.

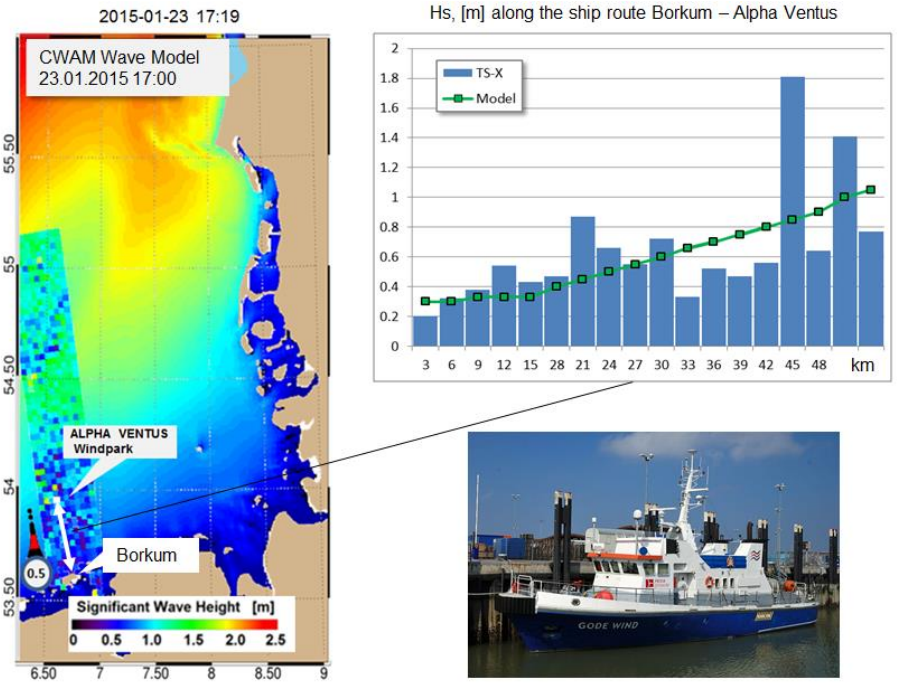

Fig.14: Validation Example. Spatial overlay of TerraSAR-X derived H_S over CWAM model results. The scene acquired on 23.01.2015 depicts a more spatially instable sea state than the model (left). The Shipping line Borkum - Alpha Ventus is shown with wave height increasing from 0.3m near the coast up to ~1m near Wind Park "Alpha Ventus". The tender vessel „Gode Wind" used for the transport of persons and materials to offshore wind farm "Alpha Ventus" (max speed 18kn ~ 30km/h) needs about 2h for this trip.

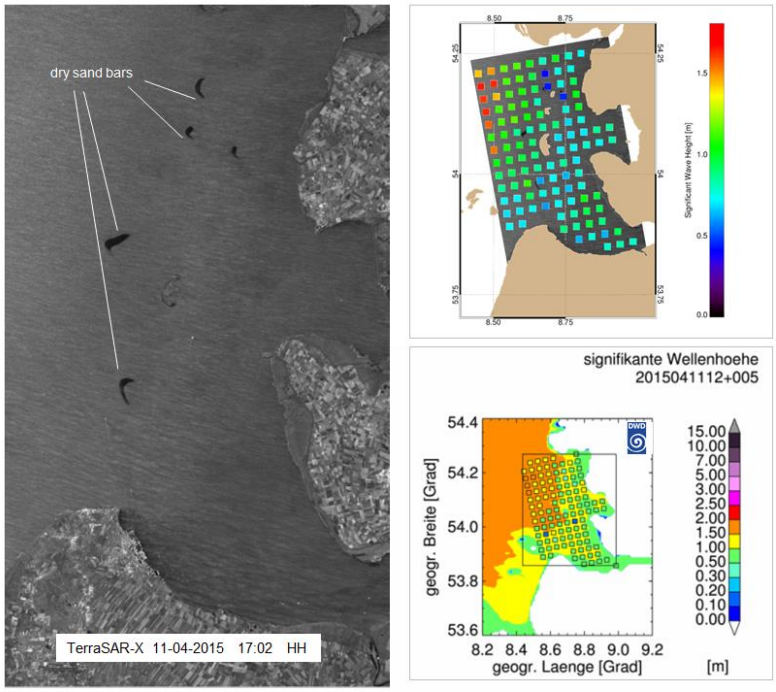

Fig.14: Validation Example. TerraSAR-X StripMap on11.04.2015 at 17:02 UTC (left) processed (top right) and plot by DWD with overlaying with CWAM model results (bottom right). Interesting to note that the sand bars apparently dry by TerraSAR-X are wet in the model with sea state H_S ~1-1.5m. In TerraSAR-X the waves are damped around the bars with H_S ~ 0.3-0.8m.

The statistics conducted for available TS-X scenes with 61 weather conditions on a local scale results in values very similar to results gained earlier for regional scale: according to former studies (Günther et al., 2007), commonly only in 0.3% of all cases the H_S value exceeds 2.5m for local wind U_{10}<12m·s^{-1} in the southern North Sea. This statistics is based on 10 years sea state reanalysis with the WAM model for the North Sea for 1990-2000 and shows a strong general dependence of the sea state on local wind.

On the other hand, the TS-X derived sea state and wind fields show strong local inhomogeneities in wind fields in the U_{10} domain 10-16 m·s^{-1} with gusts appearance that is connected to local sea state increasing. The local impact of these gusts on ocean waves increases significantly if the gust propagation speed is close to the speed of the wave groups. Strong wind energy feeding the same group for a longer time period causes a growth of the individual wave within the group and results in a resonance. In earlier studies using SAR data, it was already shown that wave groups with abnormal height in the North Sea are connected to atmospheric effects (Pleskachevsky et al., 2012). They are caused by mesoscale wind gust that are moving as an organized system across the sea and "drag" the continuously growing waves. An identical effect, but on a smaller scale, where the local wave height increases by 1-2m in kilometer-size clusters accompanied by wind gusts in the German Bight can be now observed and investigated using new techniques based on satellite-borne data. An example can be seen in Fig.13, right: moderate gale with Beaufort-7 and rough sea, level 4. The wave height of ~3m increases to up to 4.8m (very rough sea-level 5) in small clusters of ~10km directly below wind gusts (Beaufort-8, fresh gale).

Acknowledgements

This study was supported by DLR Space Agency with project DeMARINE-2 SEEGANGSMONITOR and by BMVI (German Federal Ministry of Transport and Digital Infrastructure) with project "Development of Sea-State-Monitor to improve Sea State prediction systems" N 97.0304-2012. The authors gratefully acknowledge the COSYNA data portal by HZG, NWS (North West Shelf) Portal by BSH and EMODnet for data providing.

References

Breit,H., Fritz,T., Balss,U., Lachaise, M., Niedermeier, A. and M. Vonavka (2010): ***TerraSAR-X SAR Processing and Products***. IEEE TRANSACTIONS ON GEOSCIENCE AND REMOTE SENSING, VOL. 48, NO. 2, FEBRUARY 2010. 0196-2892/$26.00 © 2009 IEEE.

Behrens, A. and H. Günther (2009): ***Operational wave prediction of extreme storms in Northern Europe.*** Nat Hazards (2009) 49:387–399, DOI 10.1007/s11069-008-9298-3.

Bruck, M, Pontes, M. T., Azevedo, E. and S. Lehner (2011): ***Study of Sea-State Variability and Wave Groupiness Using TerraSAR-X Synthetic Aperture Radar Data***. Proc. 9th EWTEC-2011, pp 1-7, 5 - 9 September 2011, Southampton, UK.

Bruck, M. and S. Lehner (2013): ***Coastal wave field extraction using TerraSAR-X data***, Journal Appl. Remote Sens. 7(1), 073694 (Sep 25, 2013).

Bruck, M. (2015): ***Sea State measurements using TerraSAR-X / TanDEM-X data***, PhD Theses, University of Kiel.

COSYNA data web portal CODM http://codm.hzg.de/codm/

Engen, G. and H. Johnson (1995): ***SAR-ocean wave inversion using image cross spectra***, IEEE Trans. Geosci. Rem. Sens., vol. 33, pp.1047-1056.

Güther, H., Tränkmann, I. and F. Kluwe (2007): ADOPT - Ocean Environment Modelling for Use in Decision Making support, report, GKSS.

Hasselmann, K., Chapron, B., Aouf, L., Ardhuin, F., Collard, F., Engen, G., Hasselmann, S., Heimbach, P., Janssen, P., Johnsen, H., Krogstad, H., Lehner, S., Li, J-G., Li, X-M., Rosenthal, W., and J. Schulz-

Stellenfleth (2012): ***The ERS SAR Wave Mode – a breakthrough in global ocean wave observations***. ERS Missions: 20 Years of Observing the Earth ESA Scientific Publications, SP-1326. ESA. pp. 1-38.

Hasselmann, K. and S. Hasselmann (1991): ***On the nonlinear mapping of anocean wave spectrum into a synthetic aperture radar image spectrum***, J. Geophys. Res., vol. 96, no. C6, pp. 10 713–10 729.

Kieser, J., Bruns., T., Behrens,A., Lehner, S. and A. Pleskachevsky (2013): ***First Studies with the High-Resolution Coupled Wave Current Model CWAM and other Aspects of the Project Sea State Monitor***, Proc. 13th international workshop on wave hindcasting and 4th coastal hazard symposium, 27 October - 1 November 2013, Banff, Canada.

Lehner, S., Pleskachevsky, A., Velotto, D., and S. Jacobsen (2013): ***Meteo-Marine Parameters and Their Variability Observed by High Resolution Satellite Radar Images***, Journal of Oceanography 26(2):80–91, http://dx.doi.org/10.5670/oceanog.2013.36.

Lehner, S., Pleskachevsky, A. and M. Bruck (2012): ***High resolution satellite measurements of coastal wind field and sea state.*** International Journal of Remote Sensing, Special Issue: Pan Ocean Remote Sensing: Connecting Regional Impacts to Global Environmental Change, Volume 33, Issue 23, 2012.

Li, X.-M., Lehner, S., and M.-X. He (2008): ***Ocean wave measurements based on satellite synthetic aperture radar (SAR) and numerical wave model (WAM) data - extreme sea state and cross sea analysis.*** International Journal of Remote Sensing, 29 (21), Seiten 6403-6416. DOI: 10.1080/01431160802175546.

Li. X., Lehner S. and W. Rosenthal (2010): ***Investigation of Ocean Surface Wave Refraction Using TerraSAR-X Data***, IEEE Transactions on Geoscience and Remote Sensing, 48 (2).

Li, X.-M. and S. Lehner (2013): ***Algorithm for sea surface wind retrieval from TerraSAR-X and TanDEM-X data***, In: Transactions on Geoscience and Remote Sensing.

Lyzenga, D. R., Shuchman, R. A. and J. D. Lyden (1985): ***SAR imaging of waves in water and ice: evidence for velocity bunching***, J. Geophys. Res., 90, 1031–1036.

Pleskachevky, A., Eppel, D. and H. Kapitza (2009): ***Interaction of Waves, Currents and Tides, and Wave-Energy Impact on the Beach Area of Sylt Island***. Ocean Dynamics. Volume 59, Issue 3 / Juni 2009.

Pleskachevsky, A., Lehner, S., and W. Rosenthal (2012): ***Storm Observations by Remote Sensing and Influences of Gustiness on Ocean Waves and on Generation of Rogue Waves***. Ocean Dynamics, Sept. 2012, Volume 62, Issue 9, pp. 1335-1351.

Pleskachevsky, A., Gebhardt, C., Rosenthal, W., Lehner, S., Hoffmann, P. Kieser, J., Bruns, T. Lindenthal, A., Jansen, F. and A. Behrens (2015): ***Satellite-based radar measurements for validation of high-resolution sea state forecast models in the German Bight***. Photogrammetry, Remote Sensing and Spatial Information Sciences, Volume XL-7/W3, 2015 36th International Symposium on Remote Sensing of Environment, 11–15 May 2015, Berlin, Germany. DOI:10.5194/isprsarchives-XL-7-W3-983-201

Schwarz, E., Krause, D., Berg, M., Daedelow, H. and H. Maass (2015): ***Near Real Time Applications for Maritime Situational Awareness.*** Remote Sensing and Spatial Information Sciences, Volume XL-7/W3, 2015 36th International Symposium on Remote Sensing of Environment, 11–15 May 2015, Berlin, Germany. DOI:10.5194/isprsarchives-XL-7-W3-999-201.

Schulz-Stellenfleth, J., Lehner, S., and D. Hoja, (2005): ***A parametric scheme for the retrieval of two-dimensional ocean wave spectra from synthetic aperture radar look cross spectra***, J. Geophys. Res., vol. 110, no. C5,pp. C05 004.1–C05 004.17, 2005, DOI: 10.1029/2004JC002822.

Schulz-Stellenfleth, J., König, T. and Lehner, S. (2007). ***An empirical approach for the retrieval of integral ocean wave parameters from synthetic aperture radar data***. J. Geophys. Res., 112, doi: 10.1029/2006JC003970.

Wiehle, S. and S. Lehner (2015): ***Automated waterline detection in the German Wadden Sea using high-resolution TerraSAR-X images***. Journal of Sensors, 2015, Seiten 1-6. Hindawi Publishing Corporation. DOI: 10.1155/2015/450857. ISSN 1687-725X.

Wiehle, S., Lehner, S. and A. Pleskachevsky (2015): ***Waterline detection and monitoring in the German Wadden Sea using high resolution satellite-based radar measurements***. In: Int. Arch. Photogramm. Remote Sens. Spatial Inf. Sci., XL-7 (W3), Seiten 1029-1033. 36th International Symposium on Remote Sensing of Environment (ISRSE), 11.-15. Mai 2015, Berlin. DOI: 10.5194/isprsarchives-XL-7-W3-1029-2015.